

## Numerical simulation on size effect of copper with nano-scale twins

WU Bo<sup>1</sup>, ZOU Na<sup>2</sup>, TAN Jian-song<sup>1</sup>, WANG Jian-ping<sup>1</sup>, PANG Ming<sup>1</sup>, HU Ding-yun<sup>1</sup>

1. Engine Engineering Center, China North Engine Research Institute, Langfang 065000, China;

2. Hebei University of Technology, Langfang Branch, Langfang 065000, China

Received 29 March 2010; accepted 5 November 2010

**Abstract:** To understand the tensile deformation of electro-deposited Cu with nano-scale twins, a numerical study was carried out based on a conventional theory of mechanism-based strain gradient plasticity (CMSG). The concept of twin lamella strengthening zone was used in terms of the cohesive interface model to simulate grain-boundary sliding and separation. The model included a number of material parameters, such as grain size, elastic modulus, plastic strain hardening exponent, initial yield stress, as well as twin lamellar distribution, which may contribute to size effects of twin layers in Cu polycrystalline. The results provide information to understand the mechanical behaviors of Cu with nano-scale growth twins.

**Key words:** copper; twins; strain gradient plasticity; size effects, numerical simulation

### 1 Introduction

Recent experimental results demonstrated that electro-deposited Cu with nano-scale twins, which was called nanocrystalline twin copper, may show ultrahigh tensile strength with considerable ductility. The microstructures of such twin Cu were characterized by transmission electron microscopy (TEM) observations. It is found that most grains are subdivided into twin/matrix lamellar structures with a high density of coherent twin boundaries (TBs)[1]. Efforts were drawn in order to understand the unusual mechanical properties of Cu with nano-twins[2–4]. Some important clues were achieved based on these experimental studies. Especially, it was found that the twin lamellar spacing or thickness was critical to control the yield and hardening of the material. However, deformation mechanisms governing the corresponding mechanical behaviors remain unclear so far.

Recently, HUANG and QU et al[5–6] established a mechanism-based strain gradient plasticity (CMSG) theory from the conventional Taylor dislocation model. It is a low-order theory that preserves the structure of classical plasticity without high-order stresses or additional boundary conditions. To understand the size effects associated with nano-twin Cu, it is necessary to

extend the model with the concept of twin lamella strengthening zone. It is also necessary to include the cohesive constitutive model so that grain-boundary sliding and separations can be simulated.

### 2 Conventional theory of mechanism-based strain gradient plasticity

#### 2.1 Constitutive relations

The CMSG constitutive relations incorporate Taylor dislocation model through the effective strain rate. For small dislocation density, Taylor dislocation model[7–9] gives the shear flow stress  $\tau$  in terms of the dislocation density  $\rho$  by

$$\tau = \alpha\mu b\sqrt{\rho} = \alpha\mu b\sqrt{\rho_s + \rho_g} \quad (1)$$

where  $\mu$  is the shear modulus;  $b$  is the magnitude of the Burgers vector;  $\alpha$  is an empirical coefficient of around 0.3 depending on the material structures and characteristic[10];  $\rho_s$  and  $\rho_g$  are densities of statistically stored dislocations (SSD) and geometrically necessary dislocations (GND)[10–11], respectively.  $\rho_s$  is accumulated by trapping each other in a random way, while  $\rho_g$  is introduced by NEY[10] to ensure the compatibility of the non-form plastic deformation. The GND density  $\rho_g$  is related to the effective plastic strain

gradient  $\eta^p$  by

$$\rho_g = \bar{r} \frac{\eta^p}{b} \quad (2)$$

where  $\bar{r}$  is the Nye-factor to reflect the effect of crystallography on the distribution of GNDs, which is around 1.90 for face-centered-cubic (FCC) polycrystals;  $\eta^p$  is the effective plastic strain gradient.

The tensile flow stress  $\sigma_{\text{flow}}$  is related to the shear stress  $\tau$  by

$$\sigma_{\text{flow}} = M\tau = M\alpha\mu b\sqrt{\rho_s + \bar{r} \frac{\eta^p}{b}} \quad (3)$$

where  $M$  is the Taylor factor which acts as an isotropic interpretation of the crystalline anisotropy at the continuum level and is about 3.06 for FCC metals. Since the effective plastic strain gradient  $\eta^p$  vanishes in uniaxial tension, the SSD density  $\rho_s$  is determined from Eq.(3) as

$$\rho_s = \left[ \frac{\sigma_y f(\varepsilon^p)}{M\alpha\mu b} \right]^2 \quad (4)$$

Then the flow stress accounting for the nonuniform plastic deformation becomes

$$\sigma_{\text{flow}} = \sqrt{\left[ \sigma_y f(\varepsilon^p) \right]^2 + M^2 \alpha^2 \bar{r} \mu^2 b \eta^p} = \sigma_y \sqrt{f^2(\varepsilon^p) + l \eta^p} \quad (5)$$

where

$$l = M^2 \bar{r} \alpha^2 \left( \frac{\mu}{\sigma_y} \right)^2 b \approx 18 \alpha^2 \left( \frac{\mu}{\sigma_y} \right)^2 b \quad (6)$$

is the intrinsic material length in strain gradient plasticity;  $\sigma_y$  is the initial yield stress;  $f$  is a non-dimensional function of plastic strain  $\varepsilon^p$  which takes the form:

$$f(\varepsilon^p) = \left( 1 + \frac{E \varepsilon^p}{\sigma_y} \right)^n \quad (7)$$

for a power-law hardening solid;  $E$  is the elastic modulus; and  $n$  is the plastic work hardening exponent ( $0 \leq n < 1$ ).

GAO et al[12] demonstrated that the power-law visco-plastic model incorporating the strain gradient effects can be applied to conventional power-law hardening if the rate-sensitivity exponent  $m$  is larger than 20. Then the plastic strain rate is expressed as

$$\dot{\varepsilon}^p = \dot{\varepsilon} \left[ \frac{\sigma_e}{\sigma_y \sqrt{f^2(\varepsilon^p) + l \eta^p}} \right]^m \quad (8)$$

where  $\dot{\varepsilon} = \sqrt{\frac{2}{3} \dot{\varepsilon}'_{ij} \dot{\varepsilon}'_{ij}}$  is the effective strain rate and  $\dot{\varepsilon}'_{ij}$

is the deviatoric strain rate.

The constitutive relation in CMSG, which only involves the conventional stress and strain, can be expressed as the stress rate  $\dot{\sigma}'_{ij}$  in terms of the strain rate:

$$\dot{\sigma}'_{ij} = K \dot{\varepsilon}_{kk} \delta_{ij} + 2\mu \left[ \dot{\varepsilon}'_{ij} - \frac{3\dot{\varepsilon}}{2\sigma_e} \left( \frac{\sigma_e}{\sigma_{\text{flow}}} \right)^m \sigma'_{ij} \right] = K \dot{\varepsilon}_{kk} \delta_{ij} + 2\mu \left\{ \dot{\varepsilon}'_{ij} - \frac{3\dot{\varepsilon}}{2\sigma_e} \left[ \frac{\sigma_e}{\sigma_y \sqrt{f^2(\varepsilon^p) + l \eta^p}} \right]^m \sigma'_{ij} \right\} \quad (9)$$

where  $K$  is the bulk modulus of elasticity;  $\sigma_e = \sqrt{\frac{3}{2} \sigma'_{ij} \sigma'_{ij}}$

is the von Mises effective stress;  $\dot{\varepsilon}_{kk}$  is the bulk strain rate and  $\delta_{ij}$  is the Kronecker delta tensor. The effective plastic strain gradient  $\eta^p$  in CMSG is defined in the same way as that in the higher-order MSG theory [13], and is given by

$$\eta^p = \int \dot{\eta}^p dt, \quad \dot{\eta}^p = \sqrt{\frac{1}{4} \dot{\eta}^p_{ijk} \dot{\eta}^p_{ijk}}, \quad \dot{\eta}^p_{ijk} = \dot{\varepsilon}^p_{ik,j} + \dot{\varepsilon}^p_{jk,i} - \dot{\varepsilon}^p_{ij,k} \quad (10)$$

where  $\dot{\varepsilon}^p_{ij}$  is the plastic strain rate in tensor form. Since the CMSG theory does not involve the higher-order stress, equilibrium equations and traction boundary conditions remain the same as those in the conventional theories.

## 2.2 Finite element analysis for CMSG

A finite element method might fail with strong strain gradient effects. However, CMSG theory is a lower-order theory which does not involve the higher-order stress so that the governing equations are essentially the same as those in the classical plasticity. An existing finite element program can be modified easily to deal with the plastic strain gradient effect in a reasonable way[14]. In the present research, a  $C^0$  plane strain element incorporating the CMSG theory in User-Material subroutine (UMAT) of the ABAQUS finite element program is implemented.

## 3 Model setup and material parameters

### 3.1 Calculation model

Fig.1(a) shows a bright field TEM image of an as-deposited Cu sample. It can be seen that the twin boundaries separate grains into nano-meter thick twin/matrix lamellar structures. The thickness of twin lamellar geometry varies from about 20 nm to 1  $\mu\text{m}$  (depending on the grain diameter). Most grains in the Cu sample with nano-scale twins are equiaxed in three dimensions. The post-deformation TEM microstructure

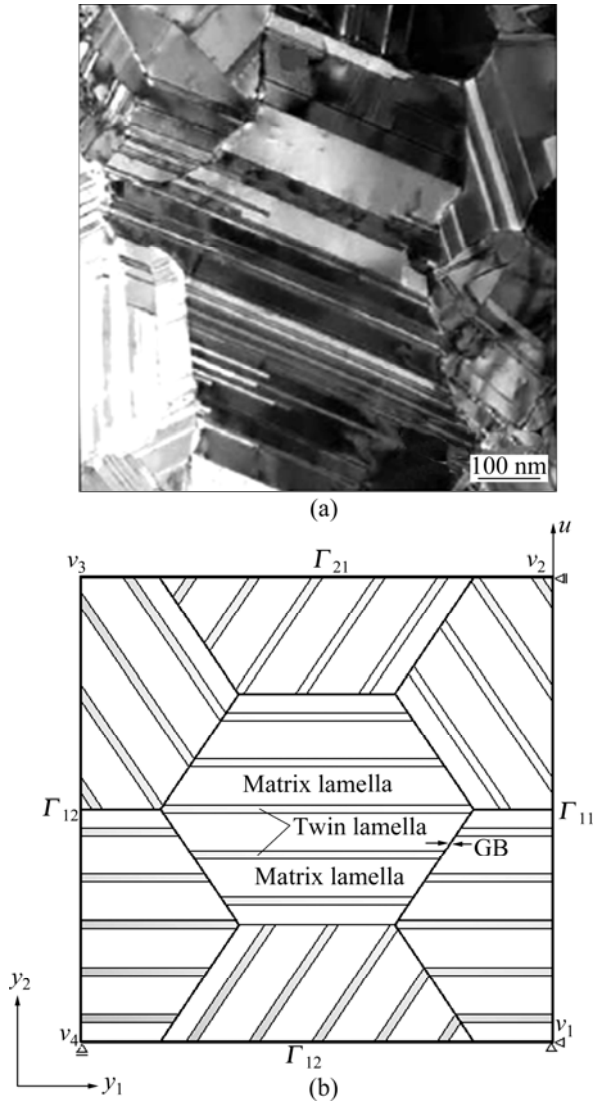


**Fig.1** Bright field TEM image [3] (a) and schematic drawing of calculation model and boundary conditions (b) of Cu with nano-scale twins

observations indicate that the interaction of dislocations with twin boundaries is crucial during plastic deformations. The dislocation configurations vary within the twin lamella thickness. For Cu with a low TB density, abundant dislocations and dislocation tangles can be seen inside thick matrix lamellae, while dislocations are hardly seen within thin twin lamellae. These observations indicate that the plastic deformation inside copper with nano-twins is extremely incompatible because of the appearance of twin lamellae, which leads to an increase in the density of geometrically necessary dislocations, as required by the plastic strain gradient (Eq.(2)). When the matrix lamellae are thicker, dislocations pile up at TBs at a certain stress concentration and the slip transmission through TBs may occur. For thin twin lamellae, a higher external stress is needed to activate dislocation reactions at TB. All these

suggest that the mechanical parameters, such as the initial yield stress and the plastic strain hardening exponent, would vary within the lamellar spacing. To handle this, it is proposed that the twin lamellae as strengthening zones have a strengthening effect on the whole deformation of the electro-deposited Cu with twin/matrix lamellar microstructure. The initial yield stresses of twin lamellae and matrix lamellae with different thickness can be calculated by the classical Hall-Petch formulism.

Fig.1(b) shows the schematic drawing of representative calculation model, where each grain contains five twin lamellae in different orientations. The representative calculation model consists of seven idealized hexagon grains, and the radius  $r$  of grain is the radius of the circumcircle of an hexagon. As displayed in Fig.1(b), the gray zones are the twin lamella strengthening zones with thickness  $d_T$ , while the white zones are the matrix lamella with thickness  $d_M$ . The cohesive interface layers with thickness  $d_{GB}$  are grain boundaries between two hexagon grains. Periodic assumption is used in the representative calculation model where the orientation of twin lamellae in all the grains is considered periodic distribution, and the periodic boundary conditions are enforced along the four sides. Here, only the final expressions are presented:

$$\mathbf{u}_{12} - \mathbf{u}_{v_4} = \mathbf{u}_{11} - \mathbf{u}_{v_1} \quad (11)$$

$$\mathbf{u}_{22} - \mathbf{u}_{v_1} = \mathbf{u}_{21} - \mathbf{u}_{v_2} \quad (12)$$

$$\mathbf{u}_{v_3} - \mathbf{u}_{v_2} = \mathbf{u}_{v_4} - \mathbf{u}_{v_1} \quad (13)$$

where  $\mathbf{u}_{ij}$  is the displacement vector for any material point on the corresponding boundary  $\Gamma_{ij}$  and  $\mathbf{u}_{v_i}$  is the displacement vector for each vertex  $v_i$ . Rigid body motions can be eliminated by requiring  $\mathbf{u}_{v_k} = 0$ , for either  $k \in \{1, 2, 4\}$ .

Both molecular dynamics simulations and direct experimental evidences suggest that grain boundary sliding and separation tend to be more important if the grain size becomes small. To include such effects, the traction-separation behavior of cohesive constitutive model is adopted as indicated in Fig.2. Here  $T$  and  $\lambda$  ( $\lambda = \delta/\delta_c$ ) are the traction stress and dimensionless separation displacement, respectively. When the grain boundary traction stress  $T$  reaches the critical value  $T_1$ , the damage is initiated and the grain boundary separation stiffness  $K_c$  descends. While the separation displacement  $\delta$  increases to the critical separation displacement  $\delta_c$ , namely  $\lambda=1$ , the grain boundary would complete the failure.

### 3.2 Material parameters

In the present analysis, to simplify the discussion of calculation results, some parameters are assumed as

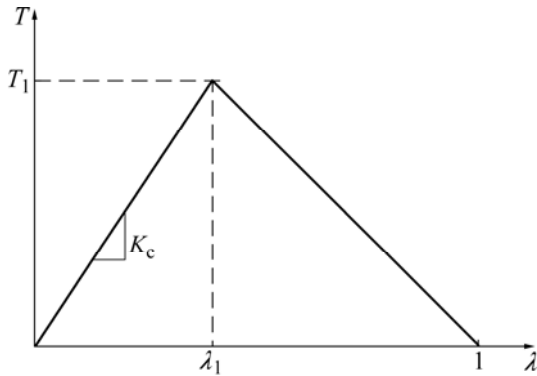


Fig.2 Cohesive force curve of cohesive model

constants or given from references, and the twin lamellar intrinsic material length  $l_T$  and the matrix lamellar initial yield stress  $\sigma_{yM}$  are taken as the normalized quantity to normalize the material parameters of nanocrystalline twin copper. The parameters dependence of the normalized stress—strain relations of Cu with nano-scale twins can be given as

$$\frac{\sigma}{\sigma_{yM}} = F \left( \frac{R}{l_T}, \frac{D_T}{l_T}, \frac{D_M}{l_T}, \frac{D_{GB}}{l_T}, \frac{E_T}{\sigma_{yM}}, \frac{K_c}{\sigma_{yM}}, \nu_T, N_T, m_T, \frac{E_M}{\sigma_{yM}}, \nu_M, \frac{\sigma_{yT}}{\sigma_{yM}}, N_M, m_M, \frac{l_M}{l_T}, \varepsilon \right) \quad (14)$$

where the subscript T and M indicate twin and matrix, respectively.

There are many parameters included in Eq.(14). For the simplification, in the present study it is considered that the material parameters  $E_M=E_T=500\sigma_{yM}$ ,  $\nu_M=\nu_T=0.3$ ,  $m_T=m_M=20$ ,  $N_T=N_M=0.2$  and  $\sigma_{yT}/\sigma_{yM}=3$ , except for some cases explained especially. Then two different size representative calculation models with grain size  $r=0.5L_T$  and  $r=5L_T$ , respectively at the same twin lamellar volume fraction are considered under axial tensile loading condition.

## 4 Results and discussion

### 4.1 Contours of Mises stress and equivalent plastic strain

The nephogram plots of Mises stresses and equivalent plastic strain for representative calculation model of nanocrystalline twin copper, in which the whole strain is 8%, are indicated in Figs.3(a) and (b). As seen from Fig.3(a), the maximum value of Mises stresses is mainly concentrated inside the twin lamella strengthening zones, especially in which twin boundaries are vertical to the tensile loading direction. Otherwise, the distribution of Mises stresses in the twin lamella strengthening zones is extremely heterogeneous,

attributing to the twin/matrix lamellae microstructures. For the incompatible deformation in the vicinity of grain boundaries, bigger Mises stresses can be also seen at the grain boundaries. Fig.3(b) shows the distribution of equivalent plastic strain when the whole strain is 8%. The bigger plastic strains are mainly in the matrix lamellae, the distributions of which form a certain angle with the tensile loading direction. The maximum value of equivalent plastic strain is concentrated in the vicinity of grain boundaries. These results are well consistent with the observation by TEM.

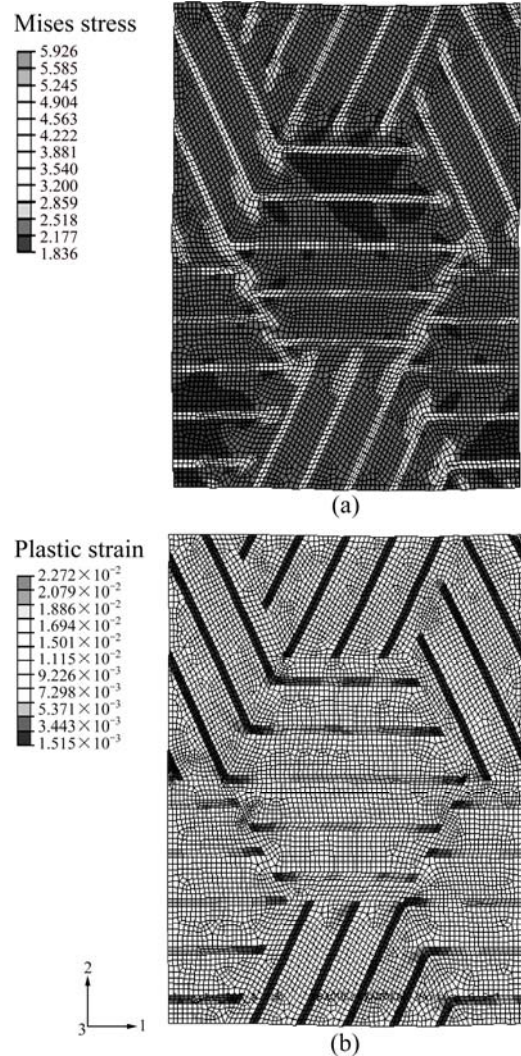


Fig.3 Mises stress (a) and equivalent plastic strain (b) nephograms of whole model

### 4.2 Stress—strain curves

Fig.4 shows the dependence of stress—strain curves of Cu with nano-scale twins on different grain size and elastic modulus. From Fig.4, it is obviously that the elastic modulus of material microstructures has strong effects on the strength of the Cu with nano-scale twins. The size effects of material become stronger with increasing elastic modulus of matrix lamellae, and the

stress—strain curves are more sensitive to the elastic modulus with decreasing grain size.

The stress—strain relations of nanocrystalline twin copper with different grain sizes and strain hardening exponents are indicated in Fig.5. As can be seen, the general mechanical properties of nanocrystalline twin copper are very sensitive to the strain hardening exponent of twin/matrix lamellae, especially when the grain size is bigger. Furthermore, with increasing strain hardening exponent, the size effects of material are much weaker.

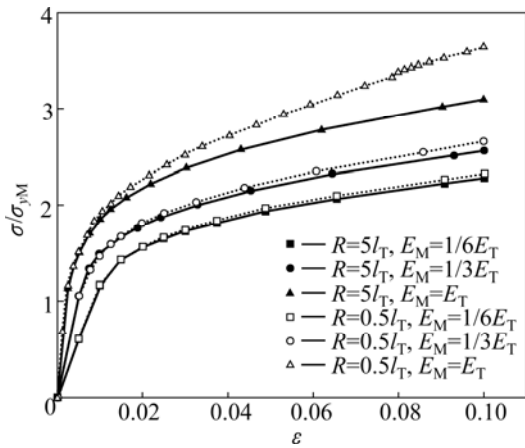


**Fig.4** Dependence of stress—strain curves of nanocrystalline twin copper on grain sizes and elastic modulus ( $E_T/\sigma_{yM}=500, m=20, \nu=0.3, \sigma_{yT}/\sigma_{yM}=3, N=0.2$ )

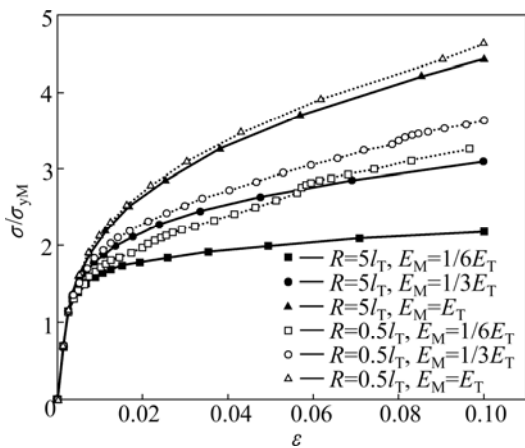


**Fig.5** Dependence of stress—strain curves of Cu with twins on grain size and plastic power hardening exponent ( $E/\sigma_{yM}=500, m=20, \nu=0.3, \sigma_{yT}/\sigma_{yM}=3$ )

The results in Fig.6 (stress is normalized by the initial yield stress of twin lamellae) show that the stress—strain curves depend on the grain size and the initial yield stress of matrix lamellae. Fig.6 shows that the initial yield stresses of twin and matrix lamellae have strong effects on the general mechanical properties and size effects of nanocrystalline twin copper. The

differences of the initial yield stresses between twin lamellae and matrix lamellae are more obvious, the size effects of material are stronger, and the influence of the initial yield stress on the stress—strain curves is smaller with decreasing grain size.

Fig.7 shows the effects of tropism distribution of twin lamellae in grains on the general mechanical properties and size effects of material. Two cases are considered, one is that the twin boundaries of all grains are vertical to the tensile loading direction, the other is that the twin boundaries of all grains become 30° to the tensile loading direction. From Fig.7, the stress—strain curves in the case which twin boundaries of all grains are vertical to the tensile loading direction are obviously higher than that in the case which is 30° in both grain sizes. Furthermore, the dependence of the general material mechanical properties on the tropism distribution of twin lamellae in grains is weaker with decreasing grain size.

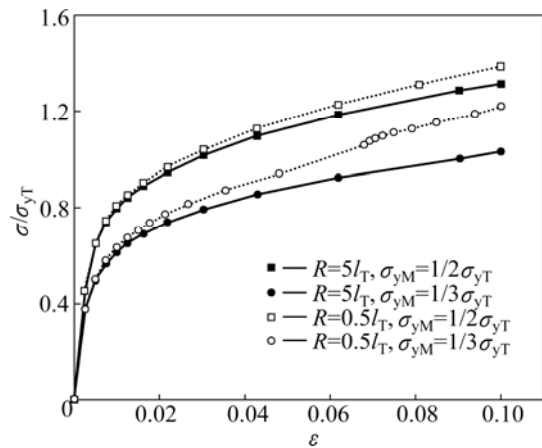


**Fig.6** Dependence of stress—strain curves of Cu with twins on grain size and initial yield stress of matrix lamellae ( $E_T/\sigma_{yT}=167, m=20, \nu=0.3, N=0.2$ )

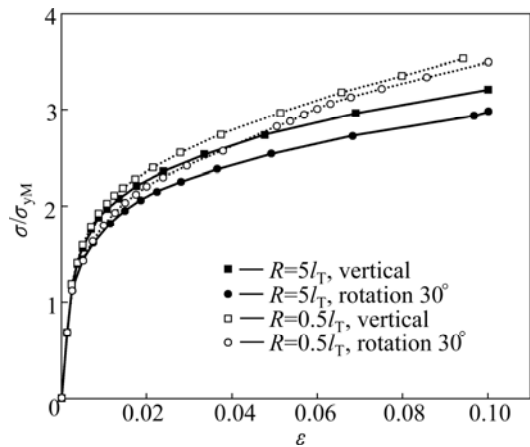


**Fig.7** Dependence of stress—strain curves of Cu with twins on grain size and distribution of twin lamellae ( $E_T/\sigma_{yM}=500, m=20, \nu=0.3, \sigma_{yT}/\sigma_{yM}=3, N=0.2$ )

### 4.3 Comparison with experimental results

The material parameters and representative calculation model geometry scales of Cu with nano-scale twins in the present analysis are obtained from the experiments of SHEN et al[2]. Both the materials of twin lamellae and matrix lamellae are copper, and some material parameters of twin lamellae and matrix lamellae are assumed, such as the elastic modulus  $E_T = E_M = 100$  GPa, the Poisson's ratio  $\nu_T = \nu_M = 0.3$ , the rate sensitivity exponent  $m_T = m_M = 20$ , the Taylor factor  $M_T = M_M = 3.06$ , the Nye-factor  $\bar{r}_T = \bar{r}_M = 1.90$ , the empirical coefficient in the Taylor dislocation Eq.(1)  $\alpha_T = \alpha_M = 0.25$ , and the magnitude of the Burgers vector  $b_T = b_M = 0.271$  nm, the average grain radius  $R$  of the experiment samples of 250 nm, and the average length scales  $D_T$  of twin lamellae in two different samples of 100 and 30 nm, respectively. Corresponding to the two different length scales of twin lamellae, the average length scales  $D_M$  of matrix lamellae are 100 and 46.6 nm, respectively. The initial yield stresses of twins lamellae and matrix lamellae with different thickness can be represented analogous to the classical Hall-Petch relation. In the present study, the initial yield stresses  $\sigma_{yT}$  of twin lamellae are 480 and 600 MPa, the initial yield stresses  $\sigma_{yM}$  of matrix lamellae are 360 and 500 MPa, respectively.

The numerical results based on CMSG of the calculation model with different twin lamellae spacing are shown in Fig.8.

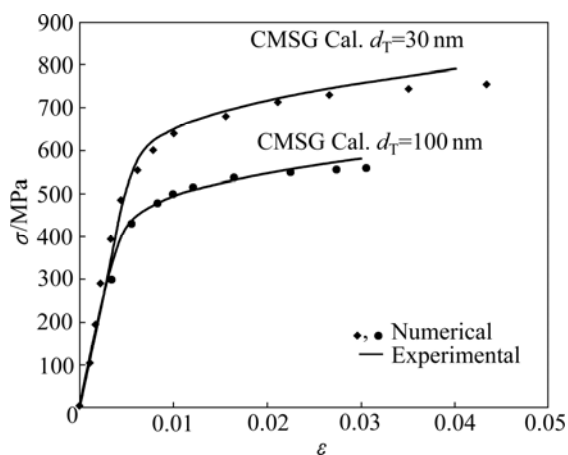


**Fig.8** Comparison between results of numerical calculation and experimental data

From Fig.8, the stress—strain curves calculated by finite element method agree well with the experimental data qualitatively and quantitatively when the strain is smaller than 2%. But when the strain value is larger than 2%, the results calculated deviate from the experimental results. Several factors may contribute to the deviation. Firstly, although two-dimensional representative calculation model (plane strain) idealization of actually

three-dimensional geometries can also preserve most important plastic deformation characteristics, the difference still exists between the model and actual materials inevitably. Secondly, the grain size and twin lamellae spacing of experimental samples are accorded with normal distribution approximately, while the geometry parameters in calculation model are the average value. Moreover, the distribution of twin lamellae in grains is assumed as periodic distribution, while the actual distribution is random. Thirdly, the strain hardening exponent of the as-deposited Cu with nano-scale twins is sensitive to the strain rate and temperature, which is not considered in the numerical calculation. Last, a perfect elastic-plastic deformation of Cu with twin/matrix lamellae microstructure is assumed and no fracture and damage are considered. Actually, the specimen always contains some damages and cracks.

## 5 Conclusions

1) The incompatible plastic deformation between twin lamellae and matrix lamellae was characterized by plastic strain gradient. Twin lamellae in Cu with nano-scale growth twins were treated as material strengthening zones and cohesive elements to simulate the grain boundaries sliding and separation.

2) The material parameters of twin/matrix lamellae, such as elastic modulus of twin lamellae and the ratio of initial yield stresses between twin lamellae and matrix lamellae, have strong effects on the general mechanical properties, the influences of which on the size effects of Cu with nano-scale twins become small with decreasing grain size.

3) The comparison between the results of numerical calculation and experimental data shows that the theoretical model adopted can well characterize the mechanical properties and size effects of nanocrystalline twin copper.

4) It is important to note that CMSG as well as other continuum plasticity theories must have lower limits and can not be applied at a scale below average dislocation spacing. Therefore, when the twin lamellar spacing is so small that the Taylor dislocation model cannot be established anymore, there may be new mechanisms of deformation such as nucleation events as shown in recent MD simulations in the as-deposited Cu with nano-scale twins that are not captured by CMSG.

## References

- [1] LU L, SHEN Yong-feng, CHEN Xian-hua, QIAN Li-hua, LU Ke. Ultrahigh strength and high electrical conductivity in copper [J]. Science, 2004, 304(4): 422–426.
- [2] SHEN Y F, LU L, LU Q H, JIN Z H, LU K. Tensile properties of copper with nano-scale twins [J]. Scripta Materialia, 2005, 52(10):

- 989–994.
- [3] MA E, WANG Y M, LU Q H, SUI M L, LU L, LU K. Strain hardening and large tensile elongation in ultrahigh-strength nano-twinned copper [J]. Applied Physics Letters, 2004, 85(21): 4932–4934.
- [4] LU L, SCHWARTER R, SHAN Z W, DAO M, LU K. SURESH S. Nano-sized twins induce high rate sensitivity of flow stress in pure copper [J]. Acta Materialia, 2005, 53(7): 2169–2179.
- [5] HUANG Y, QU S, HWANG K C, LI M, GAO H J. A conventional theory of mechanism based strain gradient plasticity [J]. International Journal of Plasticity, 2004, 20(4–5): 753–782.
- [6] QU S, HUANG Y, PHARR G M, HWANG K C. The indentation size effect in the spherical indentation of iridium: A study via the conventional theory of mechanism-based strain gradient plasticity [J]. International Journal of Plasticity, 2006, 22(7): 1265–1286.
- [7] HUANG Y, FENG X, PHARR G M, HWANG K C. A nano-indentation model for spherical indenters [J]. Modelling and Simulation in Materials Science and Engineering, 2007, 15(1): 55–262.
- [8] TAYLOR G I. Plastic strain in metals [J]. Journal of the Institute of Metals, 1938, 62(5): 307–324.
- [9] BAILEY J E, HIRSCH P B. The dislocation distribution, flows stress, and stored energy in cold-worked polycrystalline silver [J]. Philos Mag, 1960, 5(53): 485–497.
- [10] NEY J. Some geometrical relations in dislocated crystals [J]. Acta Metall Mater, 1953, 1(2): 153–162.
- [11] HUTCHINSON J W. Bounds and self-consistent estimates for creep of poly-crystalline materials [J]. Proceedings of the Royal Society of London A, 1976, 348(2): 101–127.
- [12] GAO H, HUANG Y, NIX W D, HUTCHINSON J W. Mechanism-based strain gradient plasticity (I): Theory [J]. Journal of the Mechanics and Physics of Solids, 1999, 47(6): 1239–1263.
- [13] QU S, HUANG Y, JIANG H, LIU C, WU P D, HWANG K C. Fracture analysis in the conventional theory of mechanism-based strain gradient (CMSG) plasticity [J]. International Journal of Fracture, 2004, 129(3): 199–220.
- [14] LI Xiao-yan, WEI Yue-jie, LU Lei, LU Ke, GAO Hua-jian. Dislocation nucleation governed softening and maximum strength in nano-twinned metals [J]. Nature, 2010, 464(4): 877–880.

## 纳米孪晶铜尺度效应的数值模拟

吴波<sup>1</sup>, 邹娜<sup>2</sup>, 谭建松<sup>1</sup>, 王建平<sup>1</sup>, 庞铭<sup>1</sup>, 胡定云<sup>1</sup>

1. 中国北方发动机研究所 动力工程中心, 廊坊 065000;
2. 河北工业大学 廊坊分校, 廊坊 065000

**摘要:** 为了理解电解沉积纳米孪晶铜的拉伸变形行为, 采用基于机制的应变梯度塑性理论对其拉伸变形进行数值模拟研究; 提出孪晶薄层强化带的概念, 并采用黏聚力界面模型模拟晶界的滑移和分离现象。采用的计算模型包含晶粒尺寸、弹性模量、塑性硬化指数、初始屈服应力和孪晶薄层分布等和尺度效应相关的一系列参数。计算结果有助于理解纳米孪晶铜的力学行为。

**关键词:** 铜; 孪晶; 应变梯度塑性; 尺度效应; 数值模拟

(Edited by FANG Jing-hua)